

Let there be light: illuminating physical models from the surface

David C. Henley and Joe Wong

ABSTRACT

A complex physical model (or a new seismic target) should be illuminated by seismic energy over as wide an observation aperture as possible, in order to adequately image all the details of the model. Ideally, this aperture would include 360deg of illumination of the model, and the resulting image will then accurately capture the model features for interpretation. In the field, however, we often cannot illuminate a target over more than a fraction of the ideal aperture. Hence, it is useful to explore how well we can detect and characterize the features of an unknown target using reflection data acquired over a restricted aperture, for example, data recorded on the exposed upper surface of a model, representing 90deg or less of angular range.

A complex physical model was installed at the CREWES physical modeling facility to explore illumination from various combinations of sources and receivers, including subsurface placements utilizing both vertical and horizontal boreholes. Several complete ultrasonic modeling surveys were conducted using this model. From the available data sets, we selected a multi-fold conventional 2D CMP survey and a high-spatial-resolution single-fold zero-offset survey to see how much we could observe or deduce about the physical model, using only sources and receivers located on the upper surface of the model.

Strong coherent noise appears in both data sets, and we demonstrate techniques for attenuating the noise, both on the single-fold data, and on source gathers and common-offset gathers of the conventional survey. We then form various images from each data set and discuss the model features seen on each image. Surprisingly, the single-fold high-resolution image shows more actual detail than the multi-fold stack for the shallow features, and the single-fold zero-offset image extracted from the multi-fold survey convincingly reveals the deeper model features, albeit at lower horizontal resolution.

INTRODUCTION

Physical modeling is one of the more useful techniques available for investigating many questions about seismic data acquisition and processing, particularly those associated with a specific geological structure. Because the experimenter controls many of the critical parameters of data acquisition, especially the geometry of sources and receivers, the responses of the model can provide important guidance for the design of acquisition and processing sequences for proposed seismic exploration of particular prospects.

Recently, a group of researchers at CREWES (Wong, et al, 2019) built a physical model with several subsurface features anticipated to be difficult to detect and/or illuminate with a traditional seismic survey. In particular, the presence of a near-surface high-velocity structure consisting of a sub-horizontal sill, connected at one end to a near-vertical dike, was expected to cause considerable trouble for imaging. The purpose of the model was to investigate various configurations of sources and receivers, to determine

what configuration, or combination of them, provided the most unambiguous image of the actual subsurface features. While investigating this model, not only were sources and receivers deployed along the surface, but various linear configurations of sources were placed beneath the surface, to emulate using a borehole to enhance the illumination, and hence better delineate the subsurface features. Figure 1a shows the physical model, with surface sources and receivers only, while Figure 1b shows the model with the addition of source and receiver arrays in boreholes, and Figure 1c shows the model with sources placed in vertical and horizontal boreholes, receivers on the surface. High-resolution ultrasonic surveys were performed using various combinations of source and receiver placements, some of which will be discussed in other work. However, we used only data provided by surveys which used surface sources and receivers, in order to determine what we could learn about the model from processing and displaying these surface data without recourse to subsurface sources/receivers.

We choose this approach in order to emulate a naive explorationist surveying an unknown prospect for the first time. Referring back to Figures 1b and 1c, it is obvious that some prior knowledge is required in order to properly place the subsurface sources/receivers; our analysis of the surface data is intended to show how to obtain some of that knowledge.

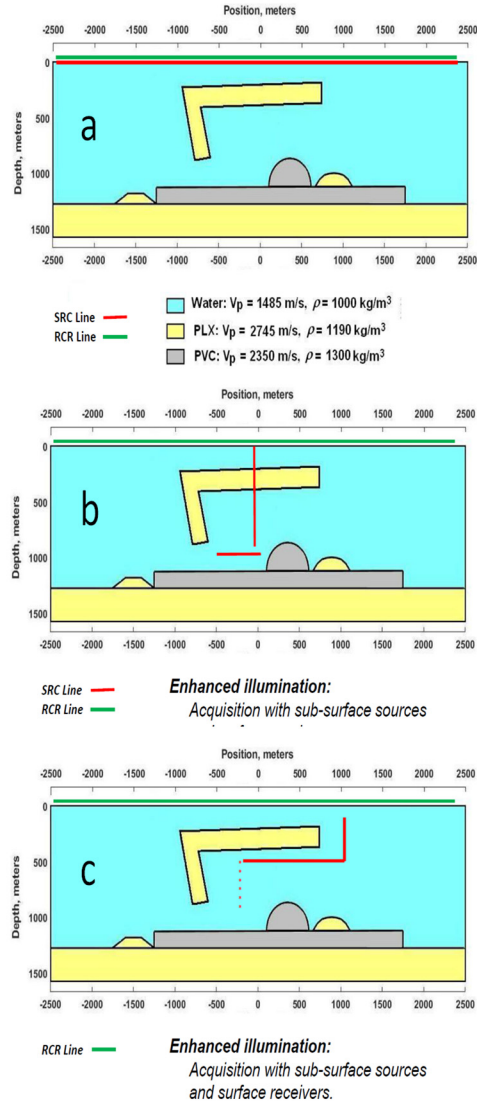


FIG. 1. Schematic cross-section of the physical model. a). Model showing surface sources and receivers only. b). Model showing one configuration of subsurface sources. c). Model showing a different configuration of subsurface sources. All dimensions shown are scaled appropriately from the actual model to field scale.

METHOD

For our analysis, we selected two specific surface surveys of the physical model shown in Figure 1. One survey is a conventional multi-fold CMP multi-offset survey consisting of 101 shots into a receiver array of 1001 receivers, all located at the surface of the model; the other is a single-fold zero-offset survey with very high lateral resolution. The latter is very reminiscent of a sonar survey; and since much of the model consists of water, including the surface layer, the comparison is quite apt. Both sets of data exhibit strong coherent reflections from the boundaries of the model, and the multi-fold survey also contains water-born direct arrivals that contaminate the reflections. In each case, we remove these artifacts as effectively as possible, then examine the data displayed in various arrangements. Our goal at each step is always to compare data images to the

details of the physical model, in order to obtain insight into what we can determine from the surface from each display.

Multi-fold survey

This survey emulates a traditional 2D multi-offset CMP survey. Each of 101 shots is fired into a spread of 1001 receivers, spaced 5m apart to yield 101 shot ensembles, each with 1001 traces, with high lateral resolution. Because of its multi-offset nature, each source gather exhibits a water-borne direct arrival event, a coherent noise that can be effectively attenuated. In addition, on any ensemble group of these traces, and on any CMP stack, the reflections from model physical boundaries are present, just as in the ‘sonar’ survey. Because the data are multi-fold, they may be presented in various single-ensemble displays, as well as stacks or ‘projections’ across common geometry coordinates, such as CMP, source, receiver, and offset. Hence, the processing applied to create various image displays of the model can include the following:

- Removal of the water-borne direct wave and related modes on source gathers
- Estimation and removal of the coherent model boundary related events on common-offset gathers.
- Application of NMO correction, using water velocity, relaxed stretch limits.
- Deconvolution of individual traces.
- Kirchhoff time migration to reduce diffractions
- Sorting to various ensembles.
- Stacking along various dimensions.
- Stacking over restricted offset ranges

Zero-offset ‘sonar’ survey

This high-resolution survey consists of 992 traces, each trace the record of a shot into the model with coincident source and receiver, using a scaled trace spacing of 5m. Because this is a single-fold survey, there is basically one way to display the traces—as a single ensemble, traces ordered from one end of the profile to the other. Subsequent processing was aimed at enhancing the image presented by the ensemble; the enhancements consisted of the following:

- Removal of strong coherent events related to the physical boundaries of the model
- Deconvolution of the individual traces to improve bandwidth
- Predictive deconvolution to remove short-period multiples

- FX deconvolution to attenuate random noise and improve lateral continuity
- Post-stack Kirchhoff migration to collapse diffractions

In order to analyze each seismic image displayed, we will present first the raw image, then the image with a schematic of the physical model superimposed, in order to see what model details are revealed in each image. In each case, the seismic image is displayed in properly scaled units of horizontal distance in metres (or dimensionless units like CMP, Source location number, or Receiver surface location number), and two-way transit time in sec. The schematics portraying the model are not displayed with any particular scale, but are simply visual aids.

RESULTS

The multi-fold survey

We begin with various displays of data from the conventional 2D multi-fold survey. Figure 2 shows a source gather from the centre position of the model. Examination of this image yields a number of prominent features. The outgoing direct arrival, which parallels the surface, is the most prominent coherent event on this record, followed by the reflection from the very bottom of the model, at about 1800ms. Prominent, high-velocity reflections from the inside surfaces of the modeling tank are also visible, but lower in amplitude. Of most interest to us, of course, are the various hyperbolic events representing reflections and diffractions generated by the details of the model itself. In order to boost the strength of these events, we applied a radial trace fan filter (Henley, 2003) to attenuate the direct wave, followed by Gabor deconvolution (Margrave, et al, 2011) to collapse the source wavelet and broaden the event spectrum, as shown in Figure 3. We then applied NMO correction, using the velocity of water and no stretch limits, resulting in Figure 4. When we overlay schematics of the model, as in Figure 5, it's difficult to directly correlate coherent events on the gather with particular features of the model, especially in the shallower part of the record.

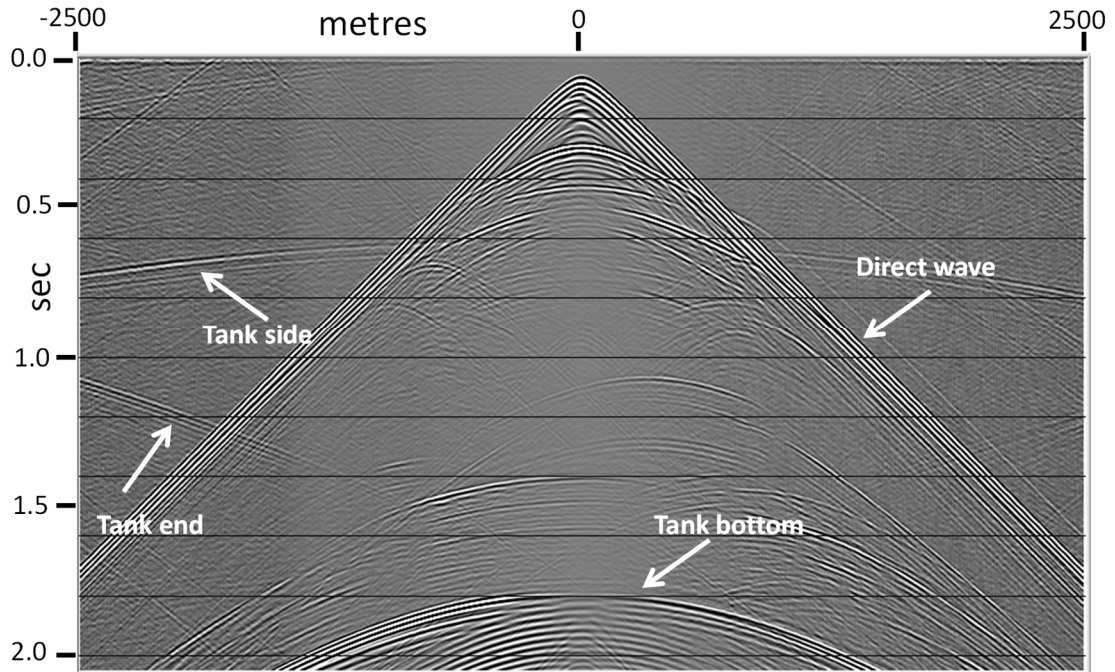


FIG. 2. Source gather for source position 501. In addition to the direct water-borne wave, strong reflections from the bottom, sides, and ends of the modeling tank can be seen. Fainter events correspond to reflections and diffractions from various model features.

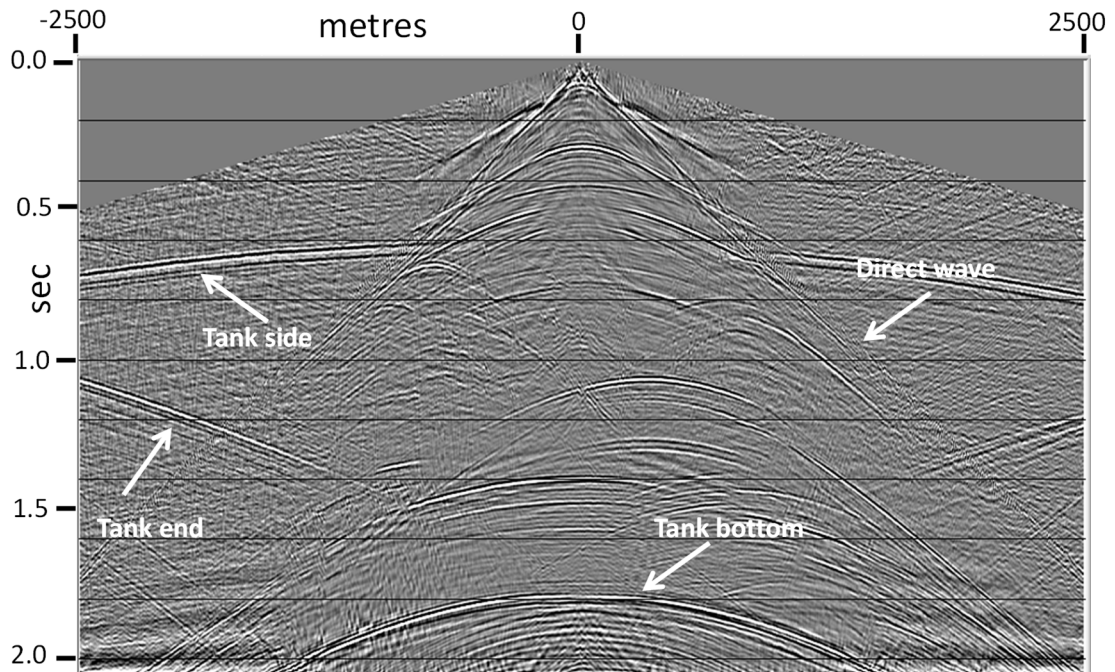


FIG. 3. Source gather from Figure 2 after application of radial trace filter to remove direct wave, and Gabor deconvolution to sharpen source wavelet.

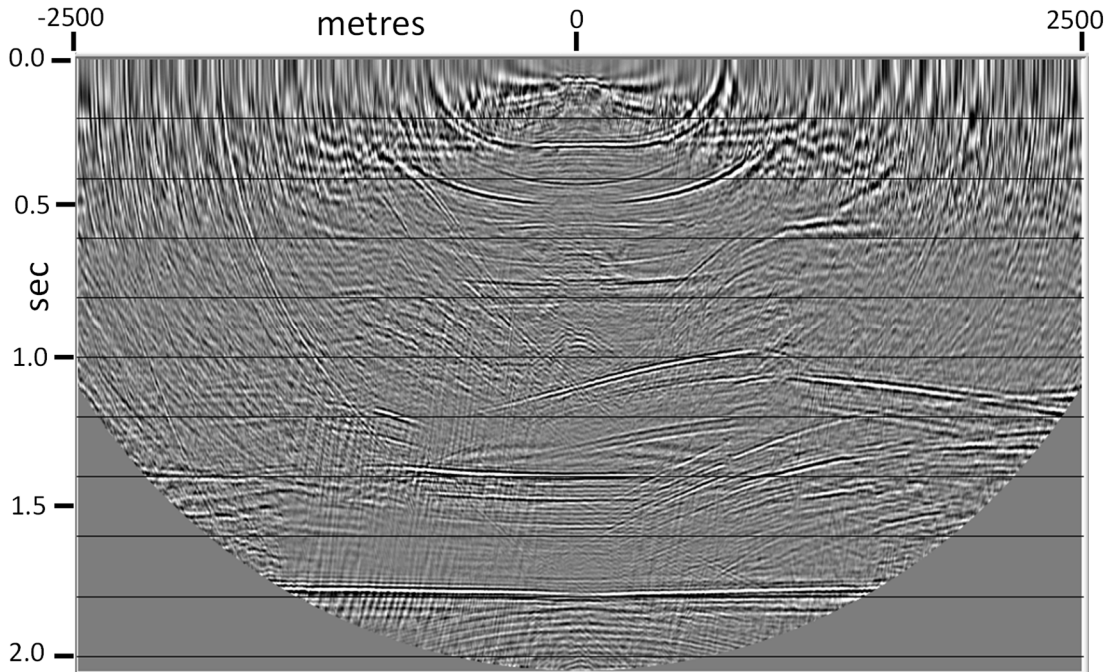


FIG. 4. Source gather from Figure 3 after application of NMO using water velocity.

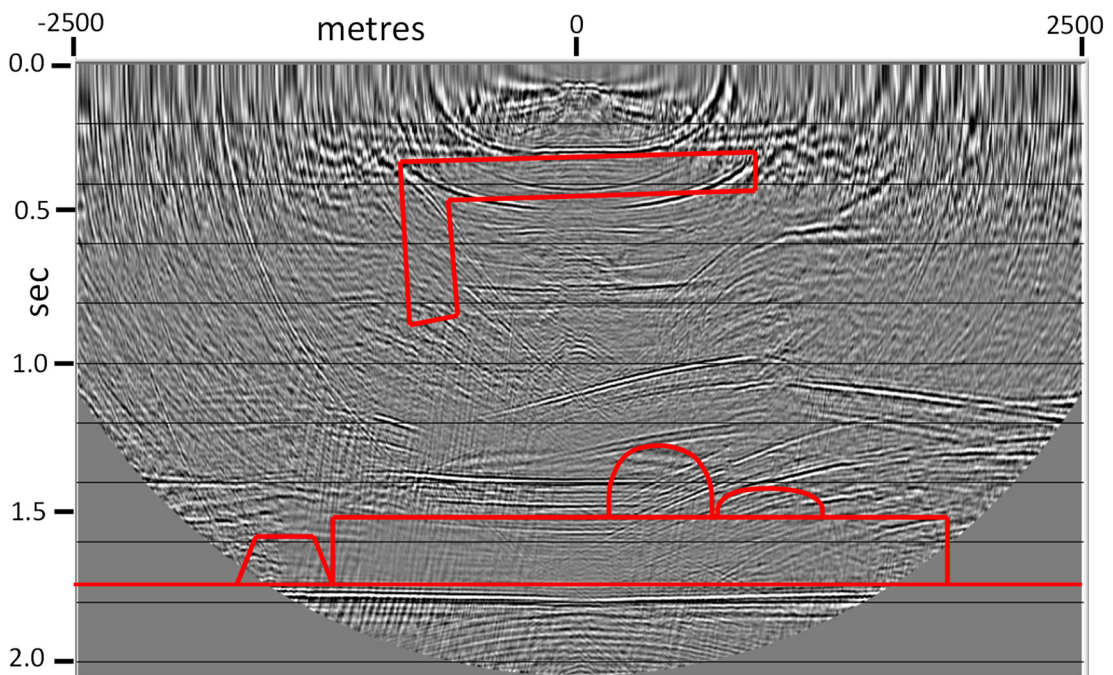


FIG. 5. Source gather from Figure 4 with schematics of the model overlaid.

We processed all 101 source gathers for the line as above, with a radial trace fan filter. The data were sorted to common-offset domain, where the tank bottom and side

reflections are horizontal. For each gather, a median mixed estimate of the side and bottom reflections was made and subtracted from the gather. Next came Gabor deconvolution, NMO correction, and CMP stacking. The result is shown in Figure 6, and with the model overlay, in Figure 7. In contrast to the single shot image in Figure 5, it is straightforward to relate most of the coherent events with various model features:

- The top surface of the shallow high-velocity layer is very well delineated, but the bottom surface is obscure.
- The only evidence of the vertical dike is a very weak reflection from its lower end.
- Diffractions and reflections correlate well with the features of the deep structure.
- A time ‘pull-up’ of the upper surface events for the deep structure, due to the shallow high-velocity layer is obvious.
- Imperfectly attenuated coherent horizontal events from the tank bottom and sides are evident, but are generally weaker than model events.
- A single linear dipping event at about 1.2 sec isn’t easily attributed to any model feature.

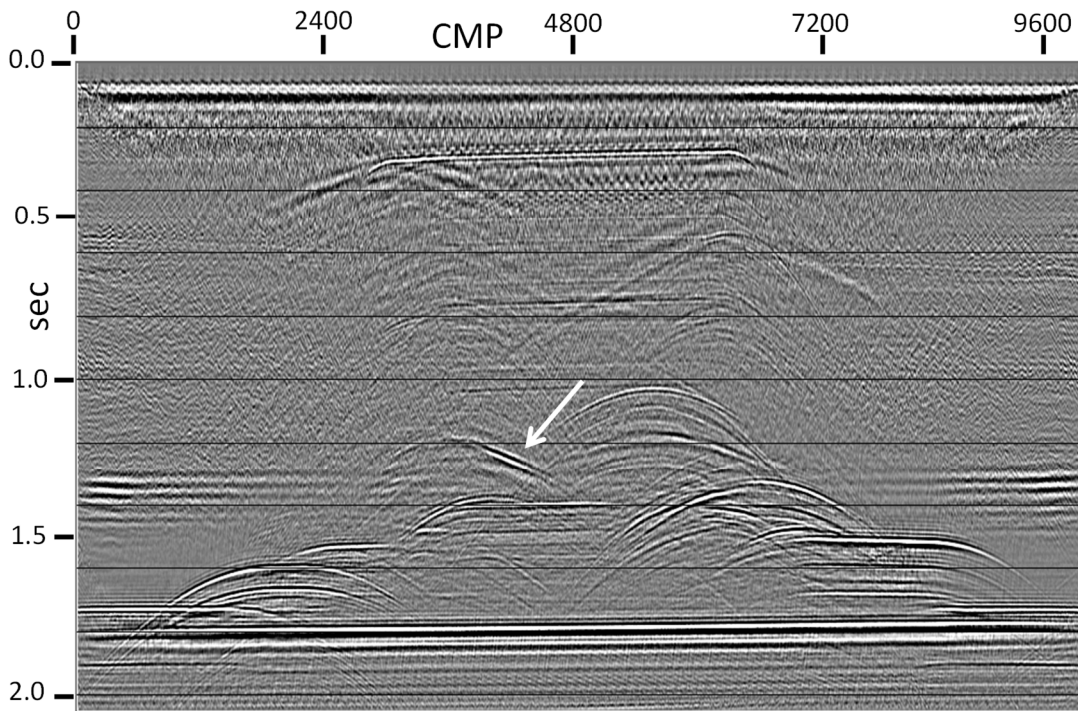


FIG. 6. CMP stack of the multi-fold survey. Arrow indicates ‘mystery’ event.

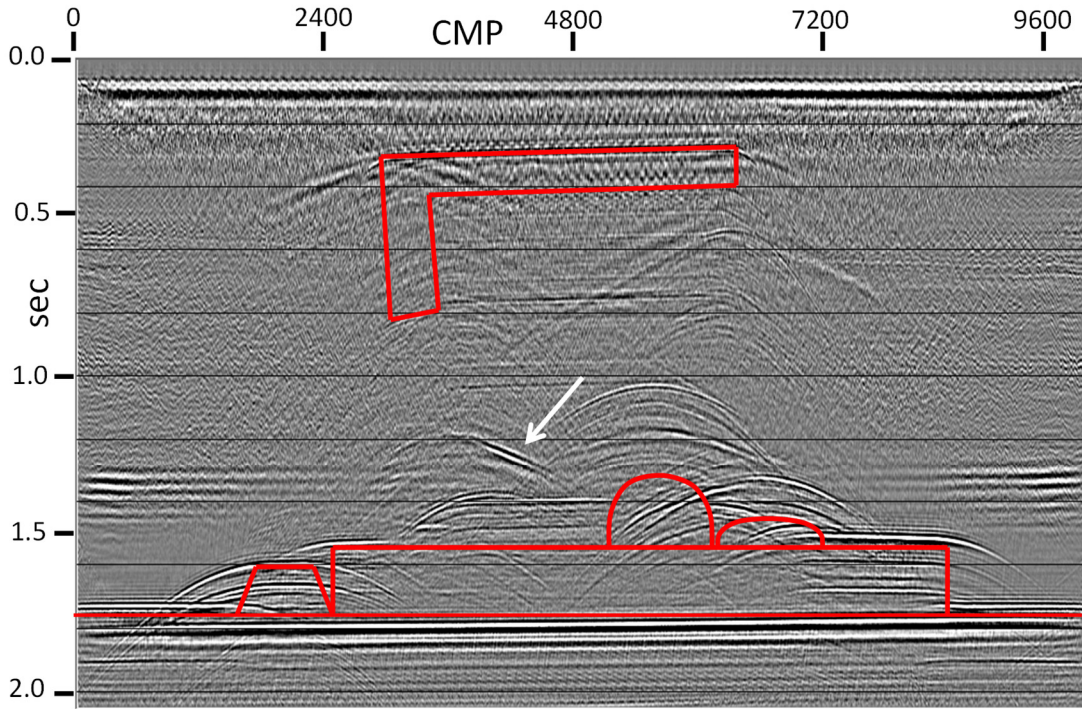


FIG. 7. CMP stack of multi-fold survey with model schematics overlaid. Arrow indicates unidentified event.

The mystery event

A single short linear event between CMPs 3620 and 4300 at about 1.2 sec is quite strong, but hasn't been directly attributed to a particular model feature. To investigate this event further, we created a set of 6 limited-offset stacks to study the raypath sensitivity of this event, as well as the events associated with various model features. Figures 8 through 13 display the CMP stacks generated for offset ranges of -1500m to -1000m, -1000m to -500m, -500m to 0m, 0m to 500m, 500m to 1000m, and 1000m to 1500m. Stacks for the longer, more oblique offsets outside these ranges were difficult to correlate to the model features, and were not included. On all the images shown, the correlation between model features and seismic events is reasonably apparent (although we had to stretch the schematic overlays to accommodate the varying trace density of the images); but only on the -1500m to -1000m and 1000m to 1500m stacks is the linear mystery event visible. This is strong evidence that offset (and hence raypath angle) is an important part of the mechanism contributing to the event. We also see that the coherent horizontal model-boundary events are strongest on the stacks with the shortest offsets (steepest raypaths) and are absent for offsets less than -1000m or greater than 1000m. This confirms that these events are reflections from the sides of the modeling tank, parallel to the survey line, and that their uncorrected moveout helps cancel them on longer-offset stacks.

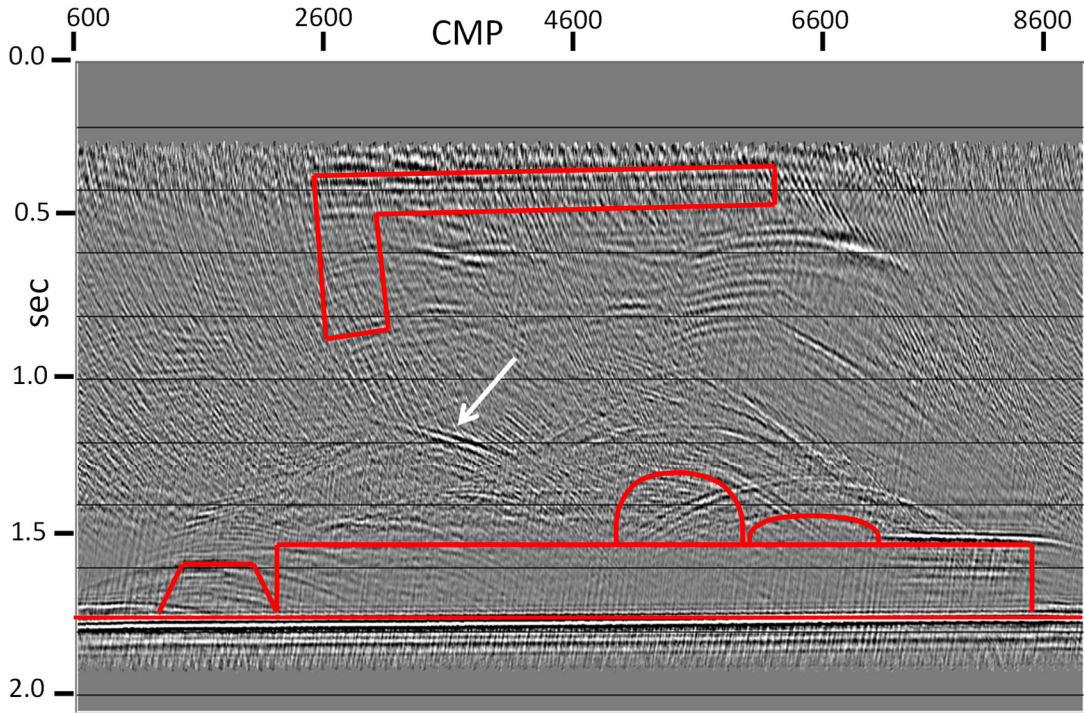


FIG. 8. Limited offset CMP stack, -1500m to -1000m. CMP range decreased because of the raypath angle. Unidentified event indicated by arrow. Tank bottom reflection visible.

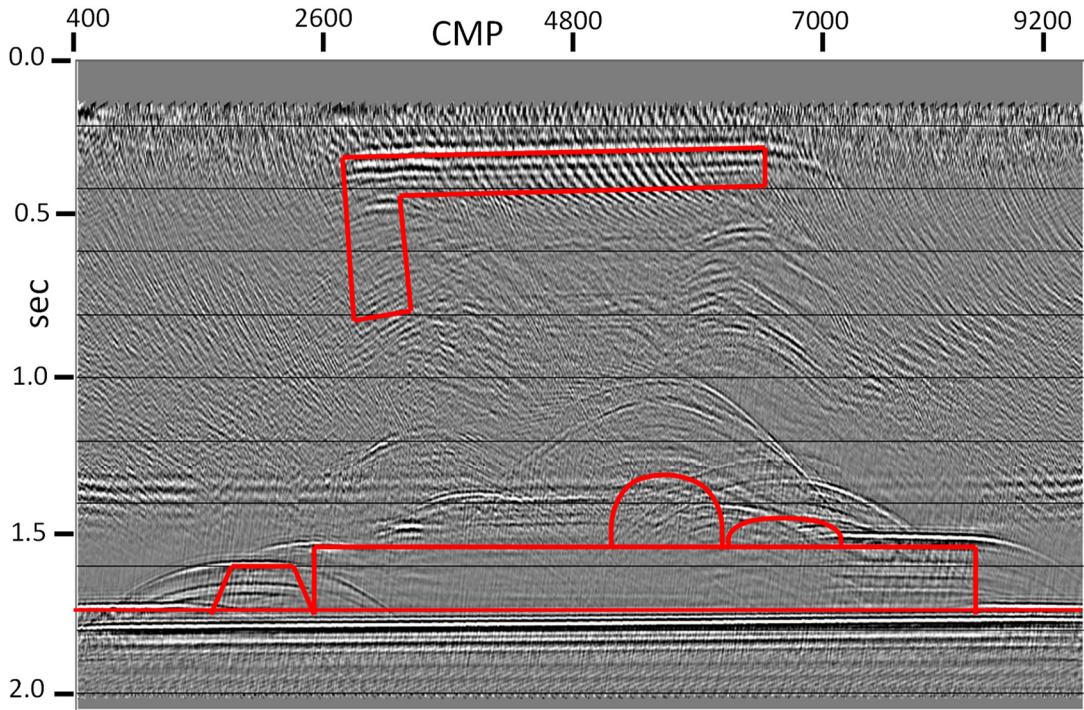


FIG. 9 Limited offset CMP stack, -1000m to -500m. Raypath angle decreases the CMP range. No unidentified event seen on this image. Tank bottom and side reflections visible.

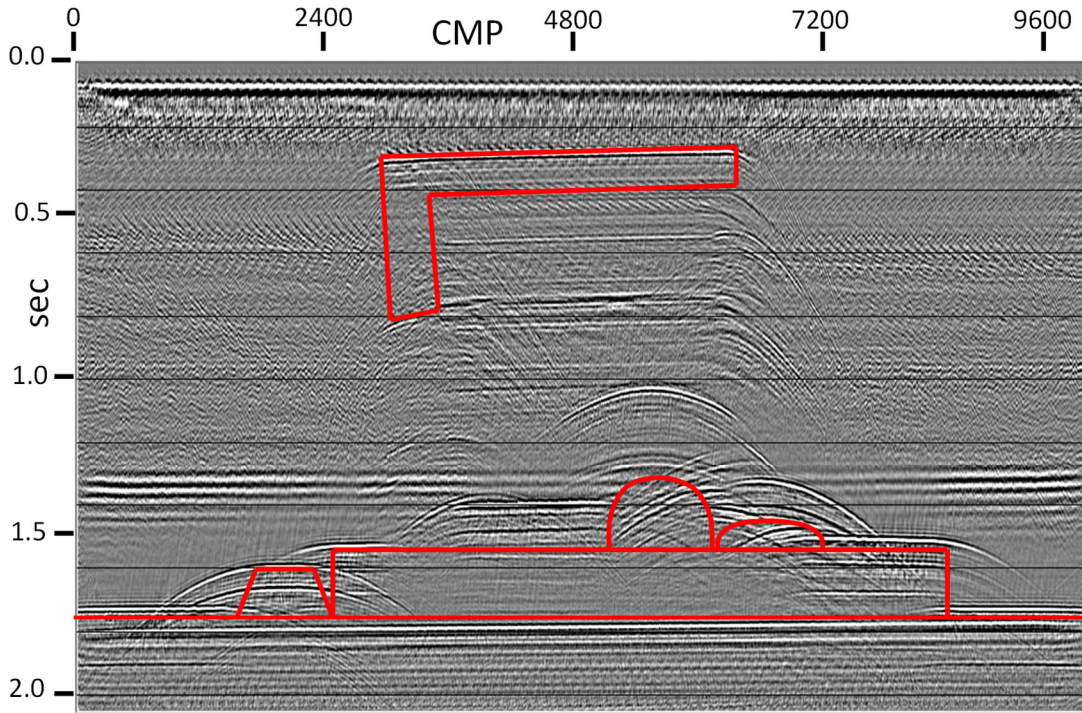


FIG. 10 Limited offset CMP stack, -500m to 0m. No unidentified event. Tank bottom and side reflections quite strong.

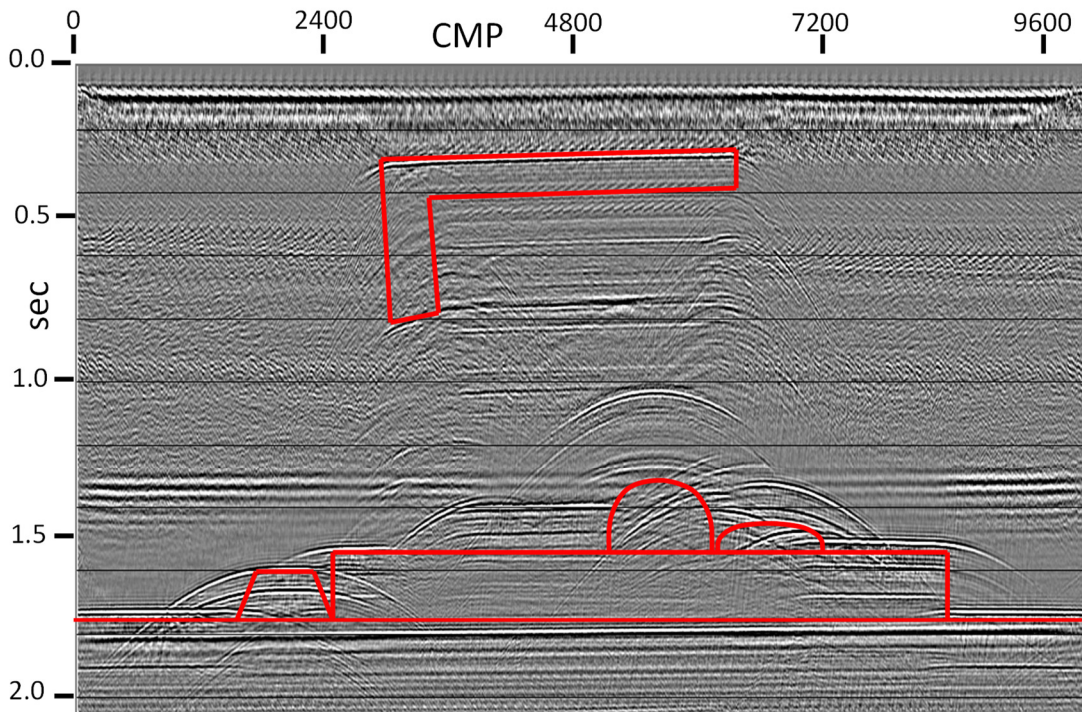


FIG. 11. Limited offset CMP stack, 0m to 500m. No unidentified event. Tank bottom and side reflections quite strong.

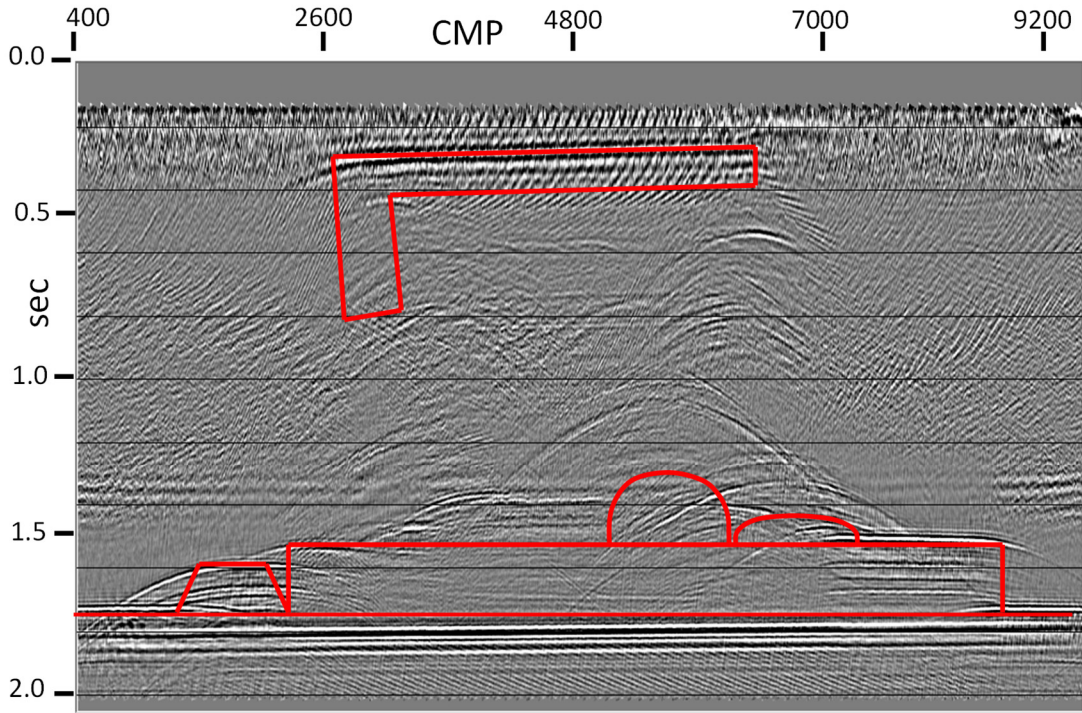


FIG. 12. Limited offset CMP stack, 500m to 1000m. No unidentified event. Tank bottom and side reflections visible.

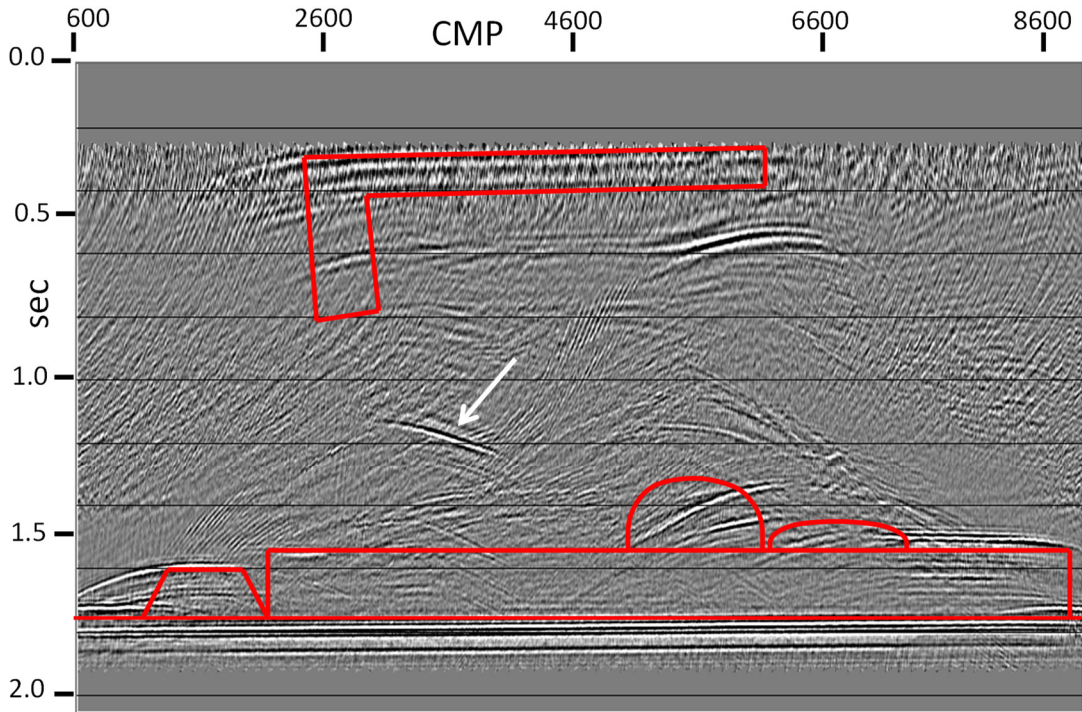


FIG. 13. Limited offset CMP stack, 1000m to 1500m. Unidentified event is quite prominent. Tank bottom reflection present.

For a more focused look at raypath-dependence of the model events, instead of limited offset stacks, we can directly examine common-offset trace gathers. We show, in Figures 14 through 18, the common-offset gathers for source-receiver offset distances of -850m, -425m, 0m, 375m, and 750m, respectively. For the zero-offset gather in Figure 16, predictive deconvolution has been applied to the traces to attenuate short-period multiples, which are particularly strong for zero offset. A close look at both Figures 14 and 18 reveals that the mystery event first identified on the CMP stack image is present on five traces in each panel, as is a dispersed event just to the left. If we overlay a schematic raypath at various positions along the model (Figures 19 and 20), where the raypath angle is determined by the offset, we observe the following:

- For a raypath as shown in Figure 19a, both legs of the raypath traverse the high-velocity sill, pulling up the reflection from the top of the model bottom slab (red arrow) by twice the time thickness of the sill (schematic is not to scale).
- The raypath position in Figure 19b traverses the sill with one leg and the full depth of the dike with the other, providing a reflection pull-up equal to the sill thickness and the dike length (arrow). Furthermore, the pulled up reflection segment is slightly tilted due to the slanted end (varying length) of the dike.
- In Figure 19c, the raypath straddles the dike, thus traversing the sill only once, and providing a pull-up equal only to the sill thickness.
- A raypath in the position shown in Figure 19d traverses the dike at a steep oblique angle, providing a pull-up that decreases as the raypath moves away from the steep wall of the dike. Because of the steep angle, part of the energy might actually be refracted along the dike wall, hence causing the ‘dispersed’ look of the pulled-up reflection.
- Figure 20a shows that a raypath corresponding to a shorter offset (narrower included angle) traverses the sill twice in the position shown, causing an unambiguous pull-up of twice the sill thickness.
- When the raypath straddles the dike, as shown in Figure 20b, it is likely that some of the energy is refracted along the dike walls; but nevertheless, there is a clear pulled-up event corresponding to the dike. Because we no longer see the ‘mystery’ event, it is clear that this raypath angle is too narrow to provide a path through the dike and the sill, as in Figure 19b. This observation provides us indirectly with information about the thickness of the dike.
- When the offset is zero, the situation is totally unambiguous. The raypath in Figure 20c traverses the sill vertically, lifting the slab reflection by twice the sill thickness.
- The raypath in Figure 20d traverses the dike vertically, pulling up the slab reflection by twice the dike length.

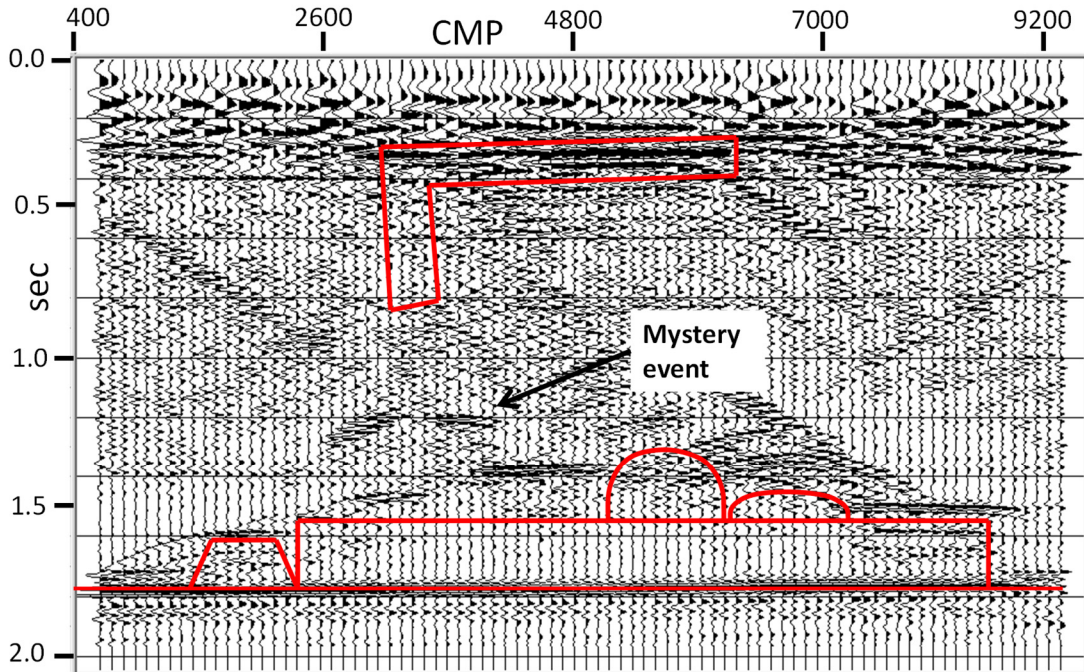


FIG. 14. Common-offset gather for offset = -850m. Mystery event is prominent.

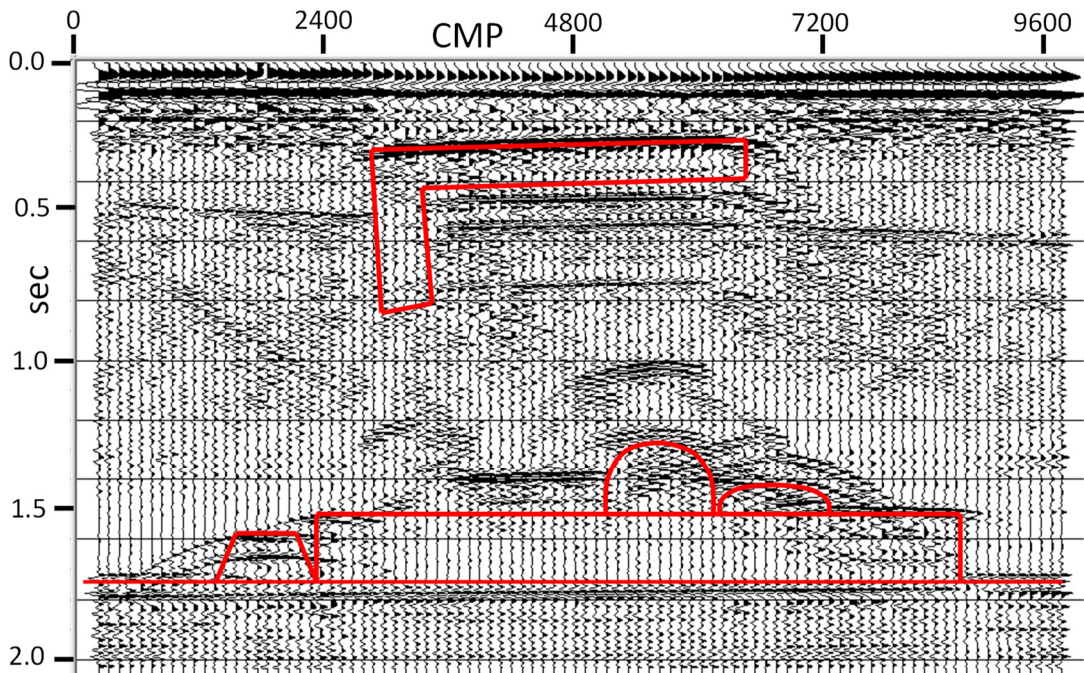


FIG. 15. Common-offset gather for offset = -425m. No mystery event.

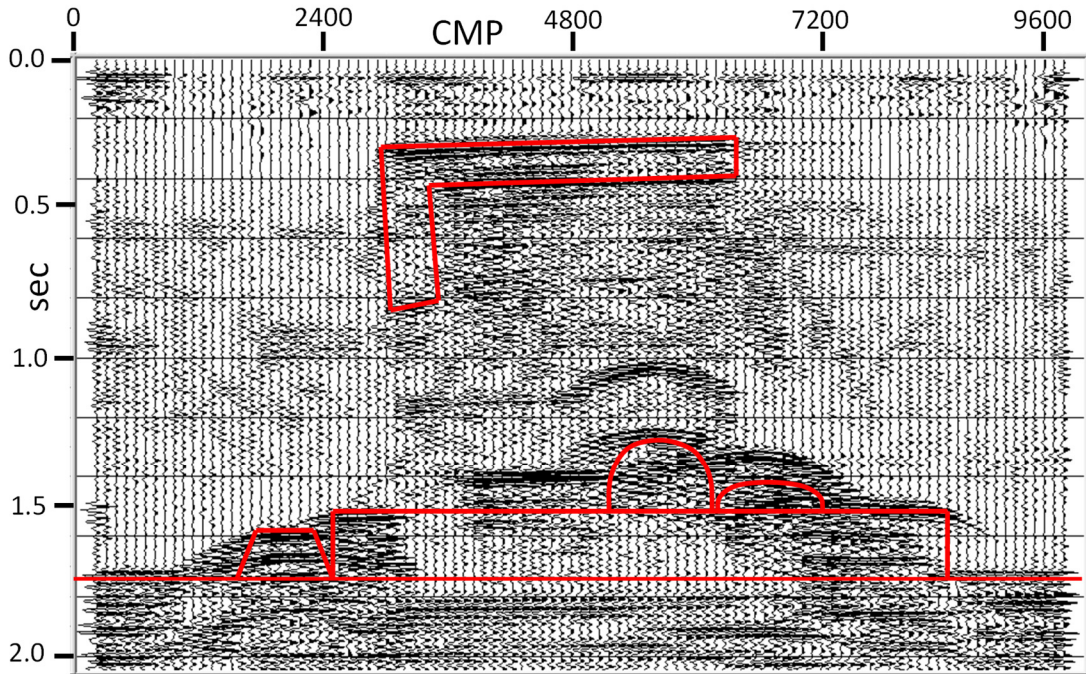


FIG. 16. Common-offset gather for offset = 0m. No mystery event.

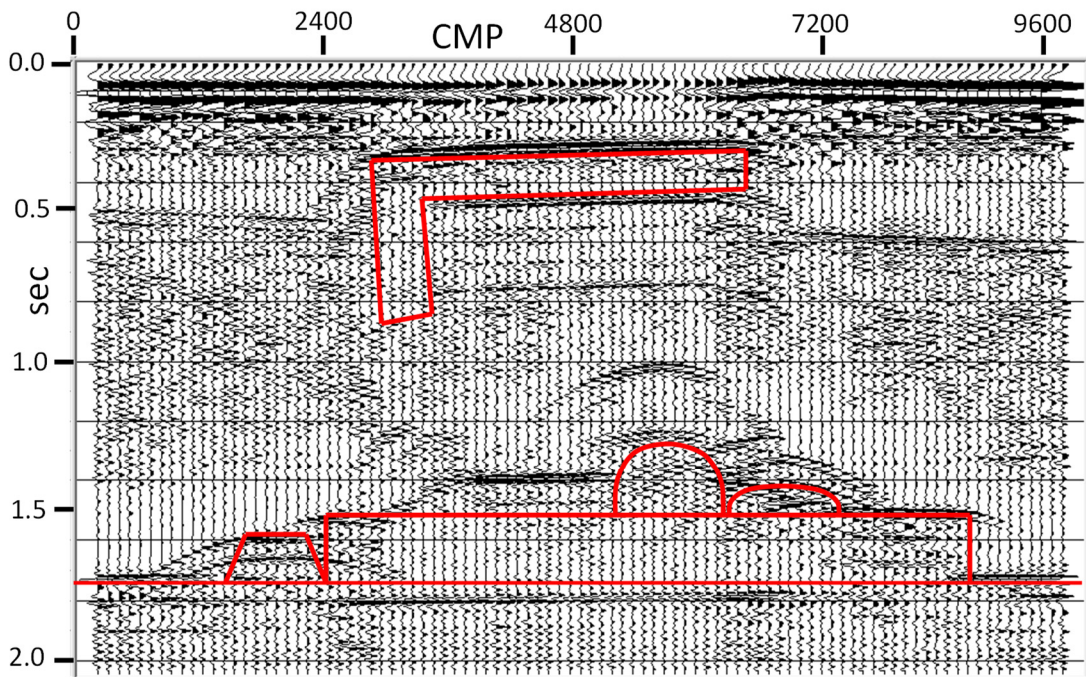


FIG. 17. Common-offset gather for offset = 325m. No mystery event.

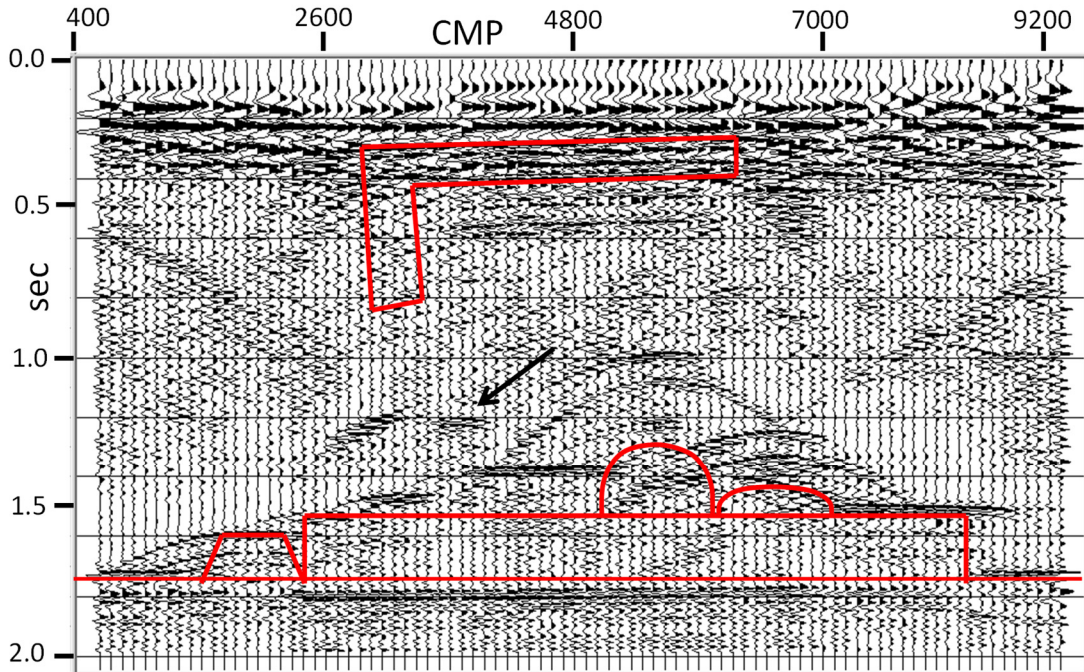
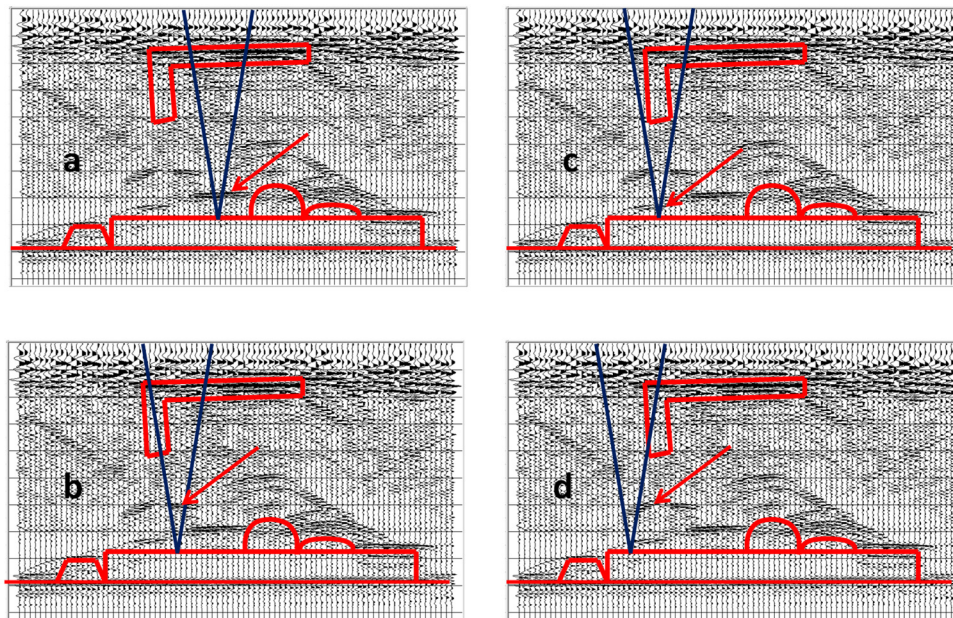


FIG. 18. Common-offset gather for offset = 750m. Mystery event is prominent.



Offset = -850m or +750

FIG. 19. a). Raypath in this position sees slab reflection through two thicknesses of the sill, causing reflection pull-up. b). Raypath here sees slab through one thickness of sill plus one thickness of dike, causing greater reflection pull-up (mystery event). c). Raypath traverses only one thickness of sill, causing small pull-up. d). Raypath traverses sill obliquely, causing large pull-up. Red arrow indicates the relevant pulled-up event in each case.

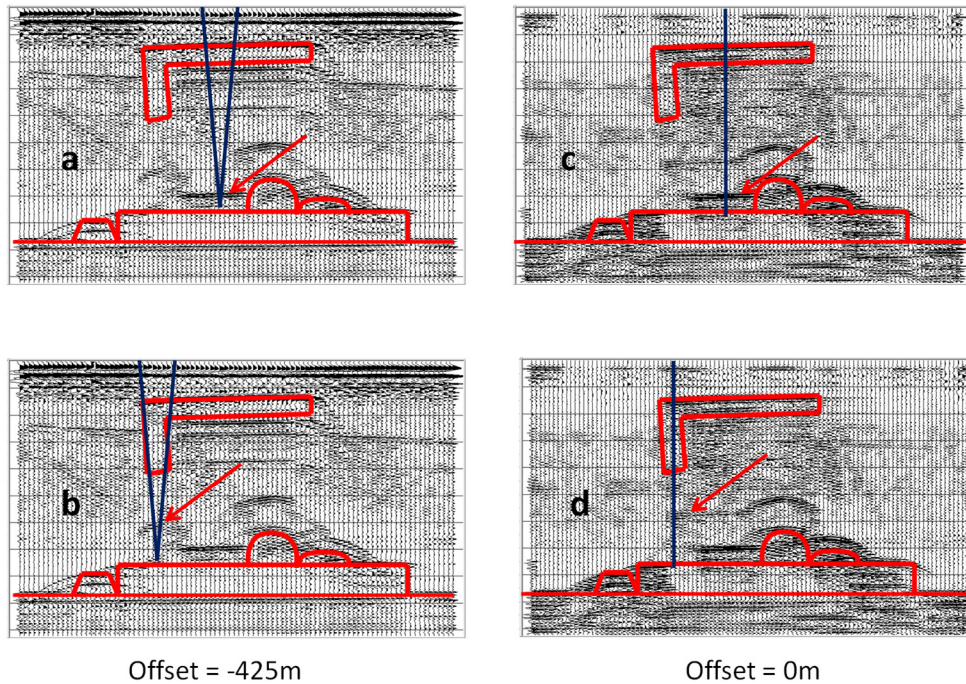


FIG. 20. a). For this offset, narrow-angle raypath in this position traverses sill twice, causing slab reflection pull-up. b). Raypath traverses sill once, only grazes dike, causing weak pull-up. c). At zero offset, vertical raypath traverses sill twice, causing pull-up. d). Vertical raypath through dike causes maximum pull-up of slab reflection. Red arrows indicate the relevant pulled-up reflections.

Other useful displays

From the basic 2D multi-fold survey, we can, of course, create many different trace displays. Above, we have used both limited-offset stacks and common-offset ensembles to identify an event in the model data whose origin was not immediately obvious. Are there other displays which could help us in distinguishing various model details? Two possibilities are the common-shot stack and the common-receiver stack, both conventionally used to isolate near-surface anomalies such as weathering anomalies. Figure 21 shows a common-shot stack, where NMO has been applied to the traces prior to stack, with the model schematics overlaid. Although various flat horizons can be recognized, the lack of diffractions hinders the recognition of edges of features and curved interfaces. Much the same comments apply to the common-receiver stack in Figure 22. One interesting feature seen in both figures is a small upward-curved event at about 1.0sec positioned just above the larger of the two dome features in the model. Comparison with other images, particularly the common-offset gathers and the various CMP stack images, shows that this event is just the reflection from the top of the dome, which has been slightly overcorrected by the NMO applied to the traces before forming the common-shot stack or common-receiver stack. Overall, these displays appear to have less utility in actually identifying model features than other images analyzed previously.

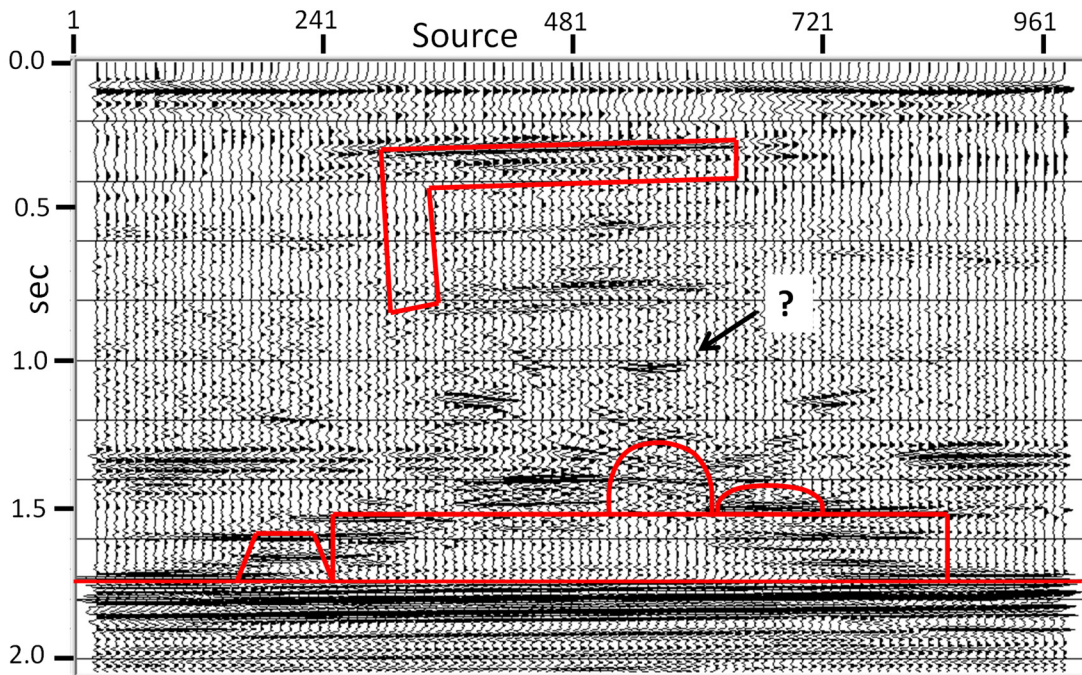


FIG. 21. Common-shot stack. Tank bottom reflection is strong, as are tank side reflections. Diffractions are missing. Arrow indicates an unidentified upward concave event. Previous mystery event is prominent.

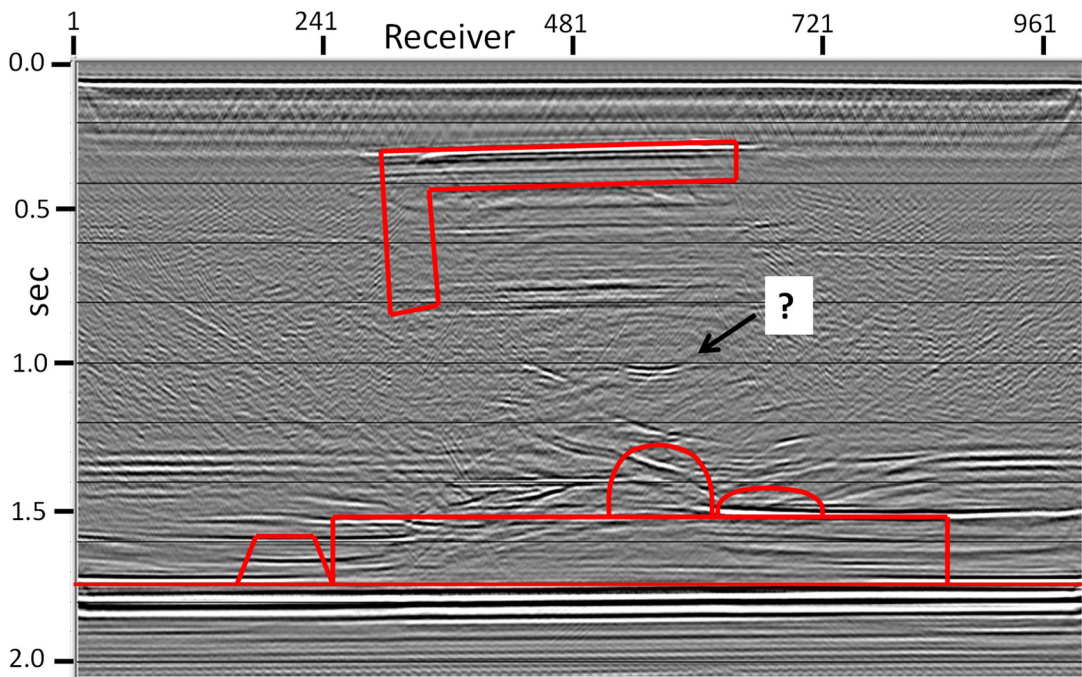


FIG. 22. Common-receiver stack. Tank bottom and side reflections are prominent. Unidentified upward concave event is prominent. This image, and the previous one, are not very informative.

The high-resolution zero-offset survey

Because of its similarity to a marine sonar survey, we will refer to this data set as the “sonar” survey. A primary objective for this data set was simply to determine how much we could learn about the physical model by examining and processing this very simple survey on its own. Since there are no source-receiver offsets, we have no chance to determine velocities in the model directly, and everything we see will be analyzed in terms of delay times alone.

Figure 23 shows a display of the raw survey traces with only AGC applied, and no attempt to attenuate noise (in this case, the horizontal events corresponding to reflections from the sides and bottom of the modeling tank). Interestingly, even on this display we can see many of the features of the physical model, including the various pulled-up segments of the base slab, and a very distinctive ‘shadow’ cast by the dike feature. A careful look even discloses a fainter shadow cast by the sill. Shadows should be no surprise, since the illumination of a sonar survey emulates that of a beam whose rays are vertical and parallel. Diffractions are present everywhere, emanating from all edges and corners of the various model features. Notably, the diffractions are much more complete than on the full CMP stack in Figure 6.

The reflections from the sides and bottom of the modeling tank can be reduced dramatically by estimating the events and subtracting them from the raw data. In our tests, a median trace mix proved most effective at estimating the events. Figure 24 shows the zero offset image after subtracting the horizontal event estimate. In this image we can now see prominent hyperbolic events originating at the edges of the model, which are almost certainly reflections from the ends of the modeling tank. We make no attempt to estimate and subtract these events, since they do not interfere with our model features. While these events also appear on source gathers in the 2D multi-fold survey, they do not survive the NMO and CMP stacking process.

The next processing step for the zero offset survey is to apply Gabor deconvolution to broaden the band and shorten the wavelet. This is shown in Figure 25. It’s interesting to see in this image that the deconvolution has also brought out new details, like diffractions from discontinuities on the upper surface of the high velocity sill. We can also see events that look like short-period interbed multiples, which can be significantly attenuated with predictive deconvolution, as in Figure 26. Applying FX deconvolution to reduce the short-period laterally incoherent noise results in Figure 27, a further minor improvement. While migration might seem to be an obvious final processing step, when we applied Kirchhoff post-stack migration to the image, the results, in Figure 28, were disappointing. The diffractions were, for the most part, collapsed; but this did not result in sharpening of model feature edges, or otherwise improve the interpretability of the image. For our purposes, we preferred the image in either Figure 26 or Figure 27.

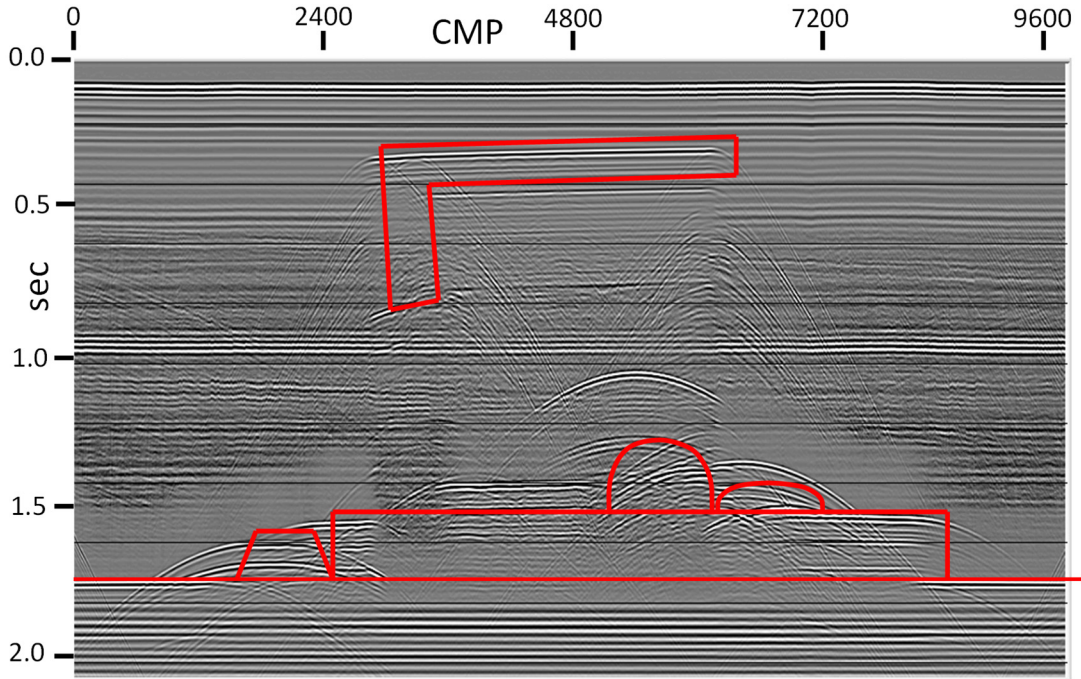


FIG. 23. Raw traces from the zero-offset 'sonar' survey. Tank bottom and side reflections are very strong.

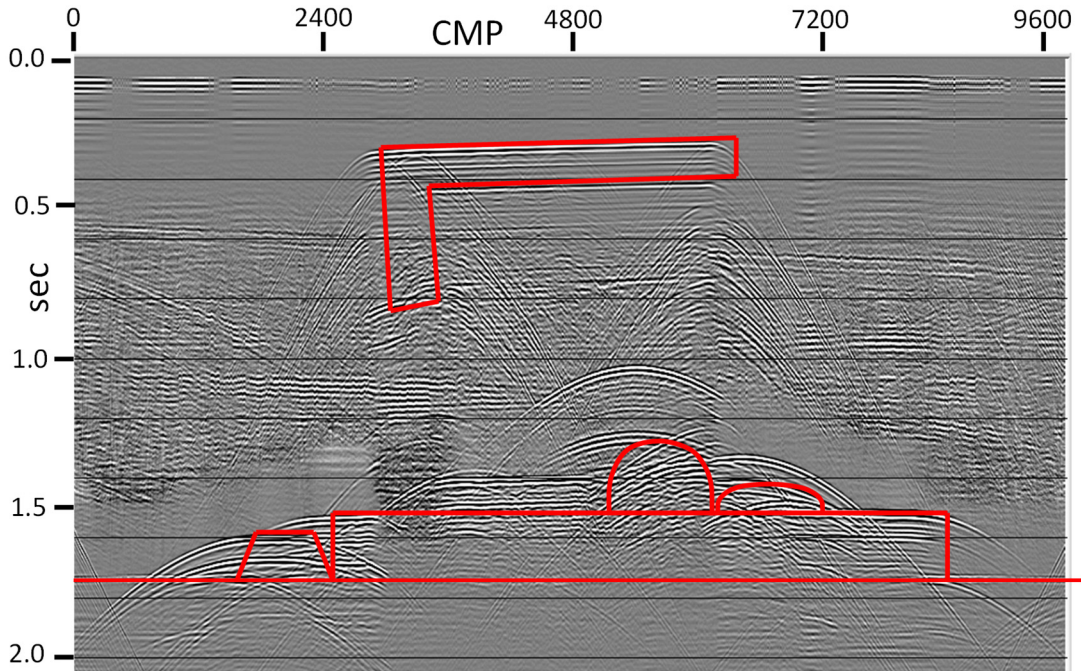


FIG. 24. Zero-offset survey with tank bottom and side reflections estimated and subtracted. Note shadow cast by the dike.

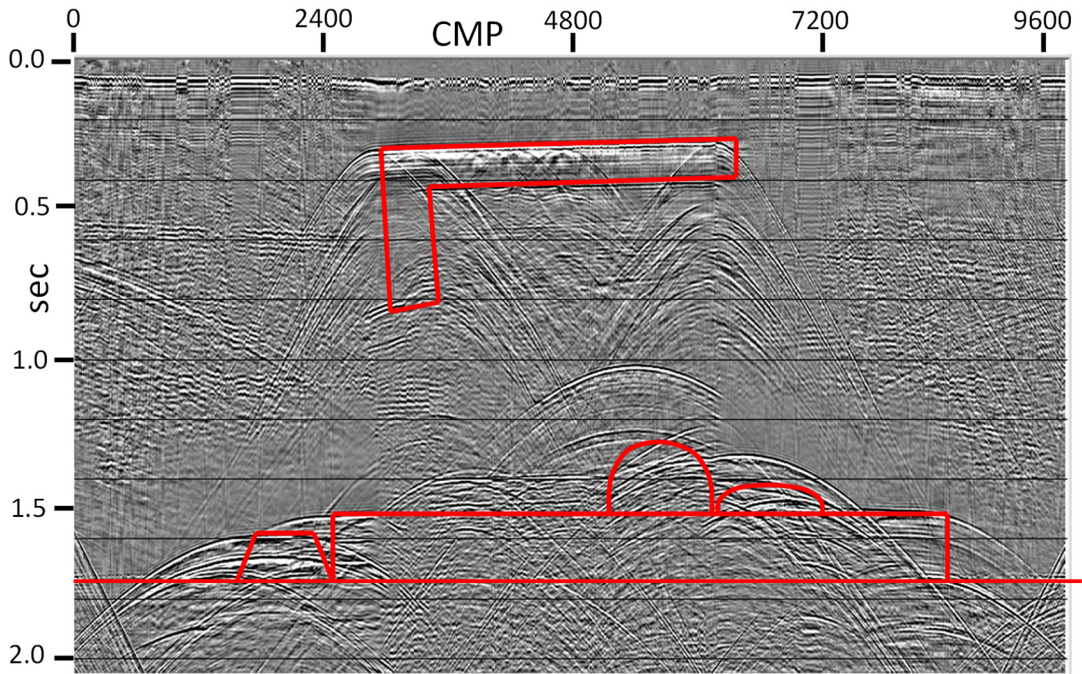


FIG. 25. Zero-offset survey from Figure 24 after application of Gabor deconvolution. New detail includes diffractions from irregularities along the top of the sill.

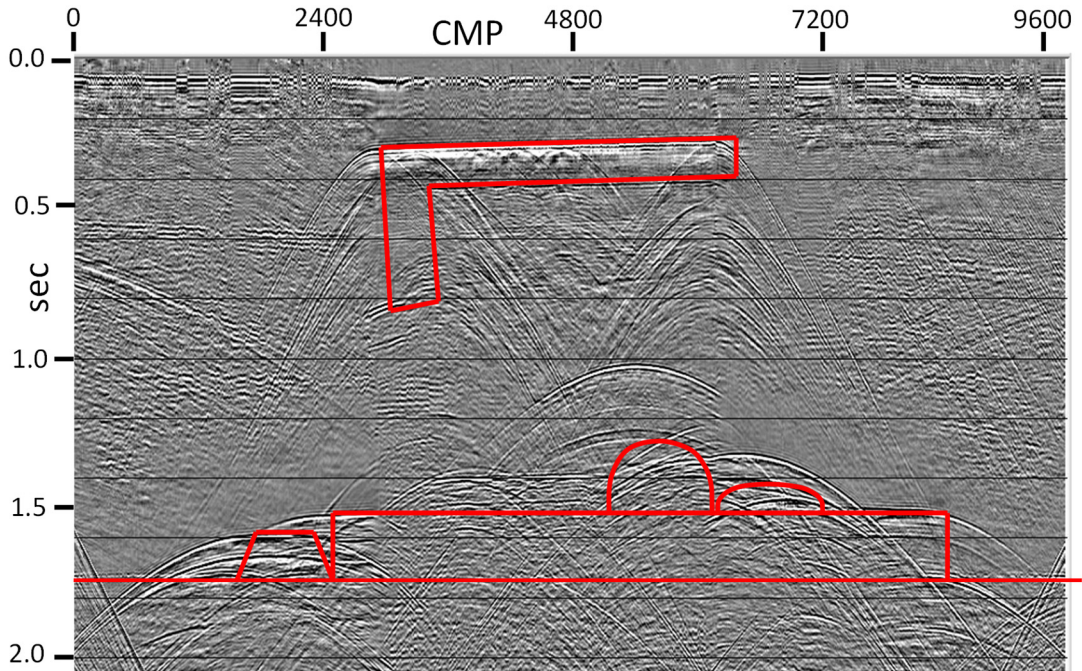


FIG. 26. Predictive deconvolution applied to the zero-offset image in Figure 25 to attenuate short-period multiples.

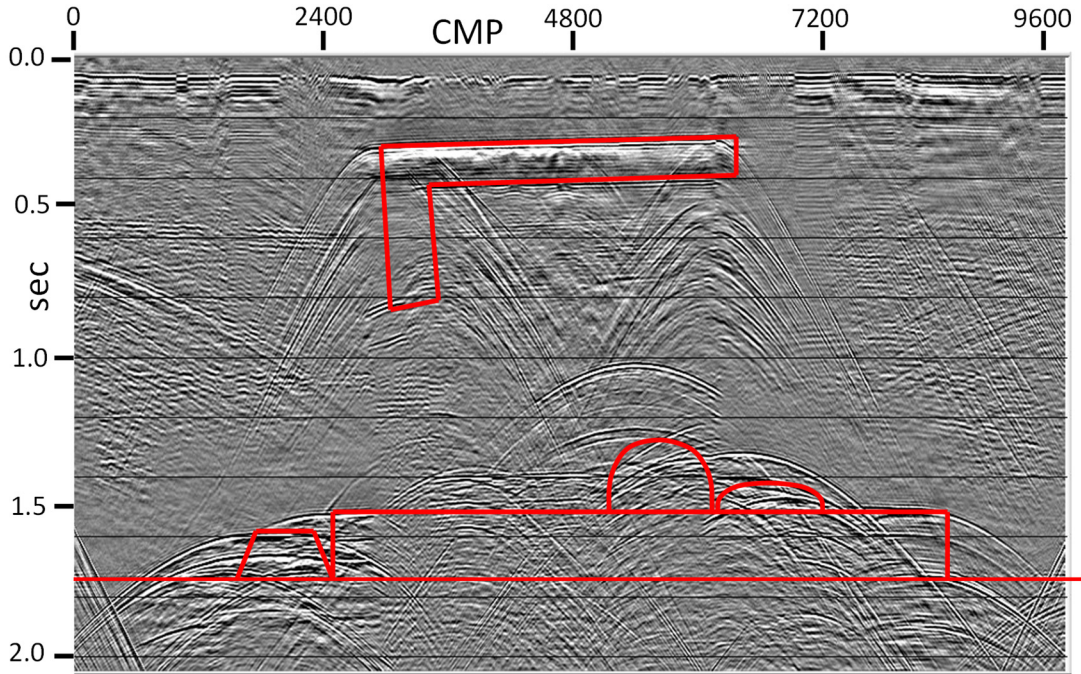


FIG. 27. FX deconvolution applied to image in Figure 26 to reduce lateral fluctuations.

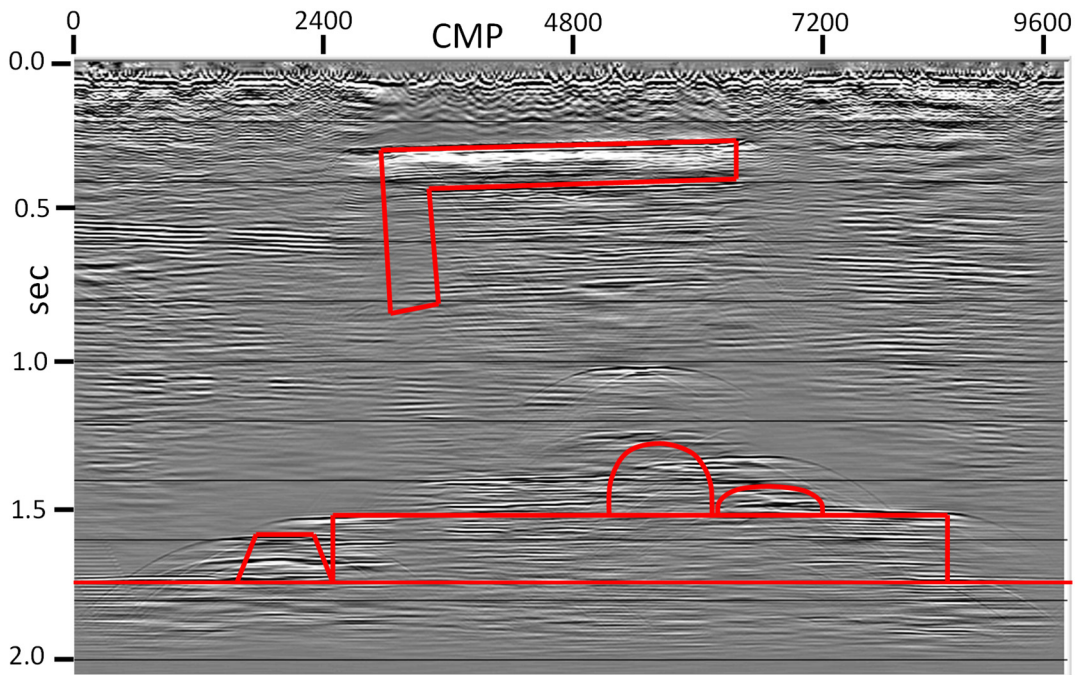


FIG. 28. Kirchhoff post-stack migration applied to the image in Figure 27, using water velocity. Diffractions have collapsed, but reflection edges not particularly enhanced. This image was deemed not very useful.

Multi-fold vs. sonar survey

As we have shown above, both the multi-fold survey and the zero-offset ‘sonar’ survey can be useful for highlighting various features of our unusual physical model. Next, we outline the most attractive features of each type of survey for the initial exploration of an unknown model.

Figure 29 is a colour display of the CMP stack of the multi-fold survey, while Figure 31 is the comparable colour display of the zero-offset survey. The CMP spacing of the stack image is 2.5m, which is half the 5m trace spacing of the zero-offset survey. A very obvious difference is the presence, in Figure 29, of not only a strong tank-bottom reflection, but the remnant of uncanceled tank-side reflections, as well. We did not apply the same median-mix estimation technique to this image as to the zero-offset survey; while this might help, it might also affect some events related to physical model features. If the multi-fold data are sorted into common-offset panels, the tank bottom and side reflections can be attenuated using the median mix estimation procedure; but since these panels are much smaller than the 992 trace zero-offset survey, the attenuation is less effective. Hence, the CMP stack process revives the tank-bottom reflection and to some extent, the tank-side reflections. The zero-offset image, on the other hand, retains the tank-end reflections which are removed in the CMP stack process for the multi-fold data. In spite of this, the diffractions from model features are much more distinct and hence carry more information in Figure 31, in spite of the coarser lateral sampling (5m vs.2.5m). One feature of the zero-offset survey that we find helpful is the fact that the dike and sill features cast distinct shadows, whose edges can easily be seen on either colour or grayscale displays. In the absence of identifiable reflections from the vertical edges of these features, the shadows can be very useful in delineating vertical interfaces.

As we would expect, the common-offset display from the multi-fold survey representing zero offset (Figure 17) shows much the same thing as Figure 31, except in much less lateral detail. While the shadow zones are still visible on this display, all the pertinent diffractions are aliased by the coarse spatial sampling.

Overall, if we had to choose between the multi-fold survey and the zero-offset ‘sonar’ survey for a quick reconnaissance, the choice would be the sonar survey. While its lateral sampling is only half that of the multi-fold survey, its constrained illumination direction (vertical) has the advantage of cleanly delineating model feature edges, and the modeling tank reflections are easily removed. Lacking multi-offset information, the survey cannot directly yield velocity information, but its detailed diffractions can be analyzed in terms of the known acquisition geometry to obtain moveout velocities for some events. While we have more access to velocity analysis with a multi-fold survey, and a better handle on coherent, source-generated noise events, we may also observe ‘mystery’ events due to particular raypaths interacting with unusual model feature configurations, such as the near-vertical ‘dike’ in our particular model. On the other hand, by sorting the multi-fold data into particular arrangements, especially common-offset gathers, we were able to identify the mystery event, and thereby obtain more information about the model feature involved. Figures 30 and 32 show both the images in Figure 29 and 31 with the model schematics overlaid, to give a final impression of how well each image reveals model details.

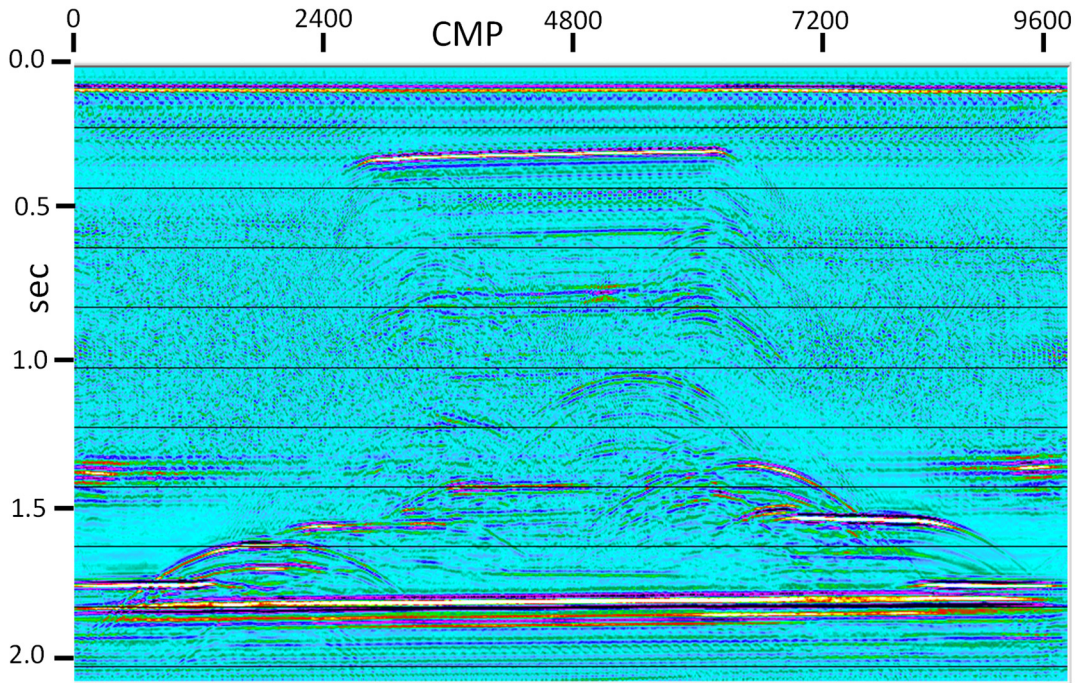


FIG. 29. Colour version of the CMP stack of the multi-fold survey. Reflections from tank bottom and sides disturb this image.

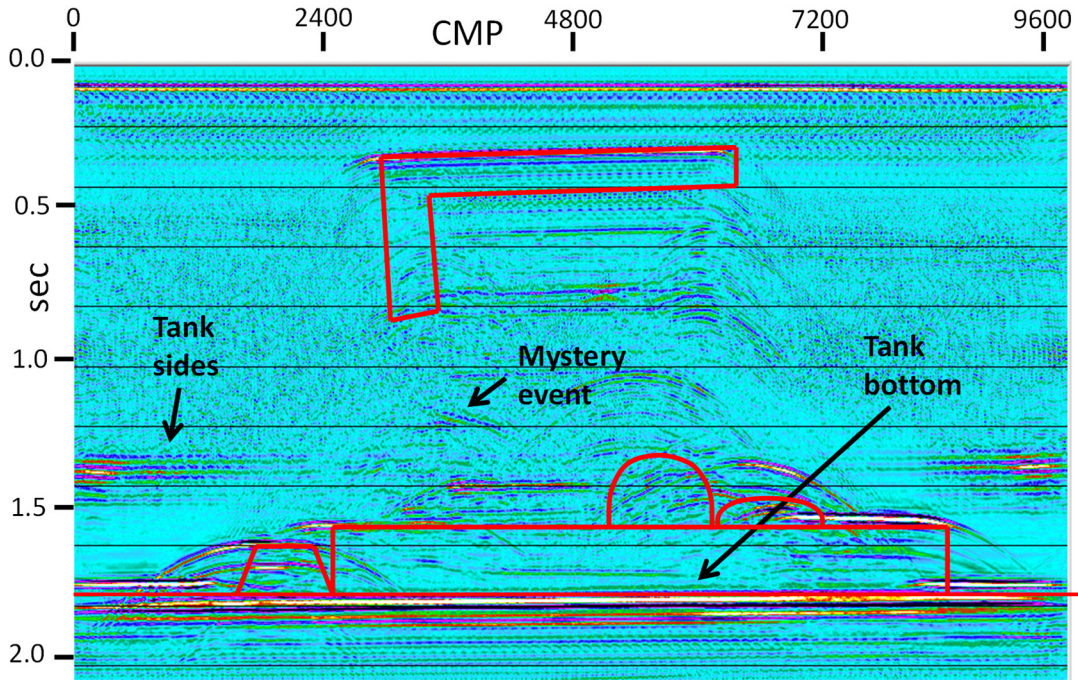


FIG. 30. Image of Figure 29 with model overlays and event identifications.

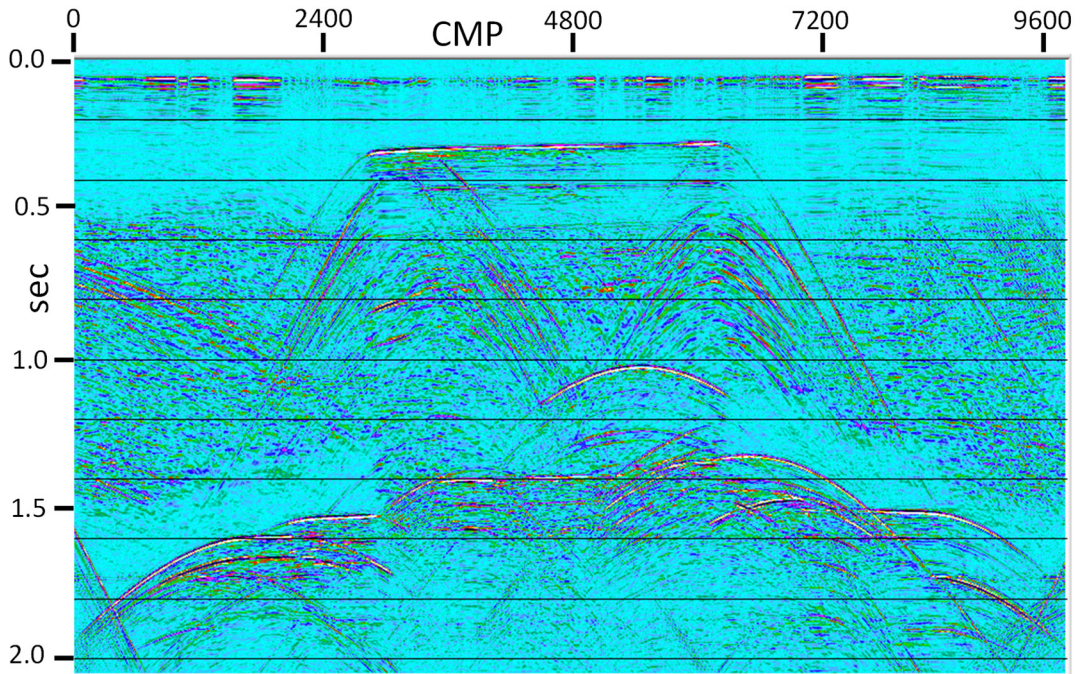


FIG. 31. Colour version of zero-offset survey. Tank end reflections visible.

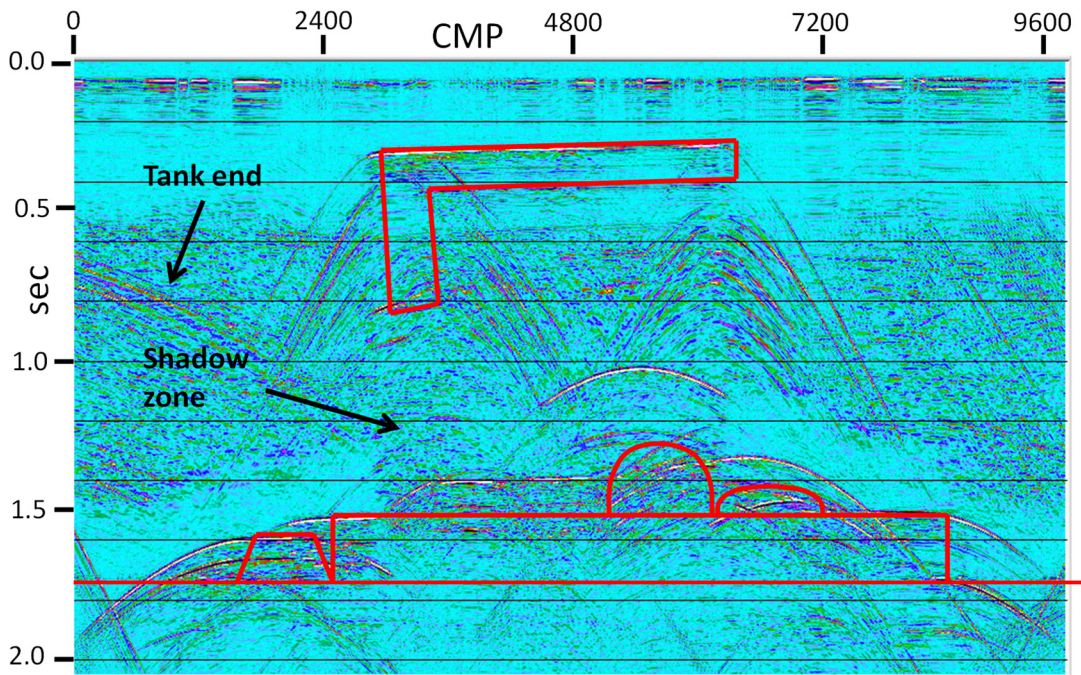


FIG. 32. Image of Figure 31 with model overlays and event identifications.

DISCUSSION

Our goal for analyzing these two data sets obtained at the CREWES modeling facility was to assess the utility of each data set for obtaining enough detail about the model to enable the possible informed placement of new subsurface sources and receivers. The preceding figures and discussion address this goal in some detail. While either the multi-fold survey or the zero-offset survey could likely be used to obtain sufficient model information, our clear preference would be the zero-offset survey because of its simplicity, not only of acquisition, but of processing and ultimately, interpretation.

Our preferences above are obviously based on modeling tank data, which have their own complications, like tank boundary reflections, but there are examples of seismic projects where surveys using very limited offset ranges but high lateral resolution have provided very useful information for use in more extensive surveys; in essence near-zero-offset surveys. One example is a set of Mackenzie Delta high-resolution surveys acquired by Shell Canada in the early 1990s, one of which we have used repeatedly in our research. Shell's stated goal in acquiring data like these was obtaining near-surface detail to assist in the processing of deeper and more complete conventional seismic surveys. The offset range for these surveys was limited to 300m, and because of the high-velocity surface, the raypaths which actually imaged deeper reflections were nearly vertical—hence nearly a zero-offset survey. The image in Figure 33 shows the CMP stack of these data after raypath interferometry (Henley, 2012). The detail in the image, even unmigrated, is remarkable and useful.

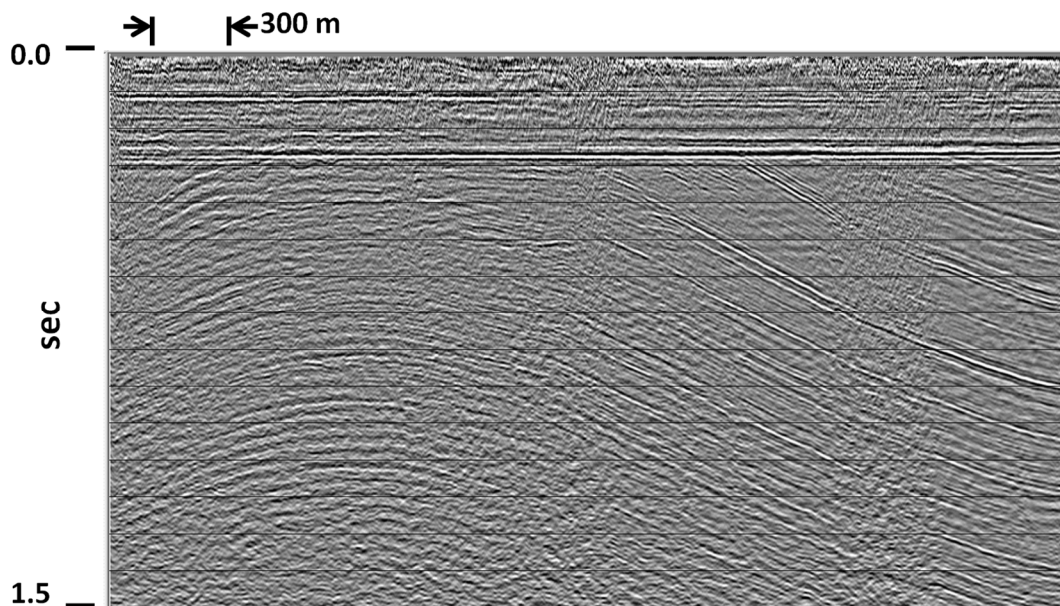


FIG. 33. This line from the MacKenzie Delta illustrates the kind of detail available in a survey that is very nearly zero-offset (because of the short, moving receiver spread and high-velocity surface layer).

CONCLUSIONS

Our main conclusion from this study is that for reconnaissance of an unknown prospect with possible complicated structural details, a high resolution zero-offset “sonar” survey is an attractive option. It has the ability to provide sharp reflections and diffractions from surfaces and edges in the structure, and because of its emulation of a parallel beam, its illumination can cast visible shadows that can be used to help delineate subsurface features. Although no overt velocity information can be obtained from the traces, the curvature of diffractions can be used to obtain some velocity information. While multiples can be an issue, most can be attenuated via predictive deconvolution. An obvious caveat for the use of a sonar survey is that data quality must be good; otherwise, the multiplicity of the multi-fold survey would work to its advantage.

While a conventional 2D multi-fold CMP stack survey can yield some of the same results, and also gives more access to velocity information, the presence of oblique raypaths leads to the possibility of reflection events which are not easily understood without ray-tracing the actual model of the structure.

Given a starting model for the structure, and using pre-stack depth migration, or some similar technique, it is likely that a 2D multi-fold survey could eventually yield a reasonably accurate image of the structure; but the simple “sonar” survey image contains enough information to accurately place boreholes and subsurface sources that could then provide the supplementary data needed for a complete image.

ACKNOWLEDGEMENTS

The authors gratefully acknowledge the financial support of both CREWES and NSERC. Thanks to Drs. Nasser Kazemi Nojadedh and Hongliang Zhang for supporting material and useful discussions. Thanks, as well, to Shell for the continuing use of their data and Halliburton for the use of donated SeisSpace software.

REFERENCES

- Henley, D.C. 2003, Coherent noise attenuation in the radial trace domain, *Geophysics*, **68**, No. 4, pp1408-1416.
- Henley, D.C., 2012, Interferometric application of static corrections, *Geophysics*, **77**, No. 1, ppQ1-Q13.
- Margrave, G.F., Lamoureux, M.P., and Henley, D.C., 2011, Gabor deconvolution: Estimating reflectivity by nonstationary deconvolution of seismic data, *Geophysics*, **76**, No. 3, ppW15-W30.
- Wong, J., Zhang, H., Kazemi, N., Bertram, K.L., Innanen, K., and Shor, R., 2019, Microseismic, SWD, and time reversal: laboratory update, CREWES research report, Volume 31.